ELSEVIER

Polymer 42 (2001) 9155–9162

polymer

www.elsevier.com/locate/polymer

Confinement induced stabilization in polymer blend thin films

Bi-min Zhang Newby[1], Katsuyuki Wakabayashi, Russell J. Composto*

Laboratory for Research on the Structure of Matter, Department of Materials Science and Engineering, University of Pennsylvania, Philadelphia, PA 19104-6272, USA

Received 12 March 2001; received in revised form 26 March 2001; accepted 26 March 2001

Abstract

Using atomic force microscopy, film stability is investigated for poly(methyl methacrylate) (PMMA)/poly(styrene-ran-acrylonitrile) (SAN) thin film blends ranging from 10 nm to a few microns thick and deposited on an oxide covered silicon substrate. In addition to characterizing the surface morphology, the PMMA rich phase which wets the surface and oxide, is selectively etched to reveal the underlying or interfacial phase morphology. For 50/50 blends at 158°C, films are found to be stable for thickness values between 20 and 100 nm. Dewetting and phase separation mechanisms are invoked to understand why films are unstable below and above this range, respectively. By annealing 25/75, 50/50 and 75/25 thin film blends between 158 and 200°C, a stability diagram is constructed and shows that blends with low PMMA volume fractions (i.e. wetting component) are more stable than blends rich in PMMA. In some cases, phase separation is observed at temperatures as low as 158°C, which is about 12°C below the bulk lower critical solution temperature (LCST). Film stability is analyzed by predicting the PMMA concentration necessary to produce a surface wetting layer at its equilibrium thickness.

Keywords: Phase morphology; Phase separation; Polymer interface

1. Introduction

Polymer thin films can be found in many industries, including microelectronics and chemical, where they are used as photo-resists in lithography and barrier coatings or adhesives, respectively. To retain their intended properties, these films are required to remain stable when exposed to various conditions, such as heat and humidity. If destabilization occurs, the film will be unable to perform as an optimum lithographic mask or adhesive layer. Destablization can occur by either phase separation, which may be confined due to thin film geometry, and/or capillary fluctuations, which lead to film rupture and eventually droplet formation [1]. Whereas prior studies have focused on characterizing the interplay between phase separation, wetting and capillary fluctuations in thin films [1], the present paper aims to understand the effect of composition and thickness on thin film stability. The stability phase diagrams will provide some guidance for technologists working with multi-component, phase separating systems.

Photo-resists, paints and adhesives typically contain a mixture of several different components, mainly polymeric. Although the bulk behavior of many blends is well known, the same blends confined to a thin film will behave very differently because of exposure to air and or substrate. To simply the problem, we will investigate a blend of a poly (methyl methacrylate) (PMMA) and poly (styrene-ran-acrylonitrile) (SAN). The system displays a lower critical solution temperature (LCST) over an accessible temperature range and its thin film behavior has been extensively studied [1]. Recent models predict confinement produces more miscible films relative to the bulk thermodynamics [2,3]. We will test this prediction experimentally. Films undergoing simultaneous phase separation and wetting can display a range of morphologies [4]. Fig. 1 shows two possible morphologies representing (a) stable and (b) unstable films with an original thickness h_0. Assuming the same phase (grey) wets both the substrate and the surface [1], a tri-layered structure or encapsulated morphology can form as shown in Fig. 1a and b, respectively. For the PMMA/SAN thin film blend, the PMMA-rich phase wets the air surface due to its lower surface energy and also wets the oxide due to a favorable acid–base interaction between PMMA and silicon oxide [5]. Film confinement and the PMMA-rich wetting layers are believed, in this study, to control thin film stability.

For 50/50 PMMA/SAN thin films ranging from 100 nm to 1 μm, three stages of phase separation have been

* Corresponding author. Tel.: +1-215-985-1386; fax: +1-215-573-2128.
E-mail address: composto@lrsm.upenn.edu (R.J. Composto).
[1] Present address: University of Akron, Akron, OH 44325, USA.

0032-3861/01/$ - see front matter
PII: S0032-3861(01)00396-2

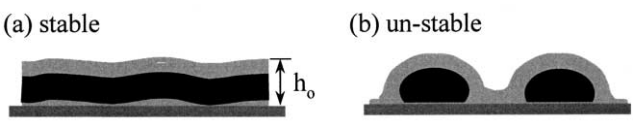

Fig. 1. Two examples of possible thin film blend structures due to phase separation and wetting. (a) A tri-layer structure, where the same component wets the substrate and air, and the other component (non-wetting) is sandwiched between the wetting layers. (b) An encapsulated morphology, where the mid-layer ruptures and forms droplets encapsulated by the wetting layer. If the tri-layer structure persists, the film is stable and has a similar thickness as the original film, h_0. If the droplet morphology forms, the film is unstable.

observed for films on homogeneous [1] and patterned [6] substrates. During the early stage, the PMMA-rich layer quickly wets both the substrate and air, and the surface layer thickness grows rapidly by hydrodynamic flow. During the intermediate stage, a tri-layer structure of PMMA-rich/SAN-rich/PMMA-rich initially forms as shown in Fig. 1a. During this stage, the minority PMMA-rich phase within the middle layer grows under 2D confinement. Eventually, the middle layer ruptures because of large amplitude capillary fluctuations. During the late stage, the ruptured mid-layer dewets from the PMMA-rich layer and forms droplets encapsulated by the PMMA-rich wetting layers as shown in Fig. 1b. In this paper, we will demonstrate that a tri-layer structure forms over a range of film thickness and composition, and most importantly, remains stable if the co-existing composition of middle SAN-rich layer can be achieved. This film is defined as stable. However, if the composition of mid-layer lies in the two phase region of the phase diagram, the middle SAN-rich layer will rupture as phase separation proceeds, resulting in an encapsulated morphology. Such a film is defined as unstable.

The objective of this study is to determine a stability diagram for PMMA/SAN thin films as a function of thickness and composition. In this paper, AFM will be used to characterize the surface and interface morphology of 50/50 PMMA/SAN thin films annealed at 158°C. Selective etching of the PMMA-rich phase allows for a unique perspective of the underlying morphology (i.e. non-wetting phase). Using the roughness from these measurements, we will define the stable and the unstable thickness range for 50/50 films. The surface and interfacial roughness for 25/75 and 75/25 thin films will also be reported and a 'stability diagram' will be constructed for each thickness investigated. The stability diagram will be interpreted by analyzing the PMMA composition within the middle SAN-rich layer and determining, using the thickness of the PMMA-rich surface wetting layer, whether this composition lies in the one or two phase region.

2. Experimental

The materials are (PMMA) and (SAN) with an AN content of 33 wt%. The specification and purification of the polymers have been described elsewhere [6]. The PMMA/SAN blends with compositions of 25, 50, and 75 wt% of PMMA are dissolved in methyl isobutyl ketone. These blends are denoted as 25/75, 50/50 and 75/25 and have a bulk critical composition near 50/50. The PMMA/SAN blend exhibits a LCST with a bulk critical temperature around 170°C [6–11]. Solutions with various concentrations of solvent are spun coated onto silicon wafers to prepare films with different thickness. These films are preannealed inside a vacuum oven at ~110°C for 16 h, and the film thickness is measured by an ellipsometer (AutoEL II from Rudolph Technologies, Inc.). The samples are then annealed at temperatures ranging from 158 to 200°C. At high temperatures, the morphology remained constant after 15 days. At the lowest temperature, 158°C, annealing for 40 days resulted in the final morphology. The samples were then analyzed using tapping mode AFM (DI 3000, Digital Instrument) before and after the PMMA-rich phase was selectively removed. Selective etching was performed by first irradiating films with 2.0 MeV He^{++} ions with an integrated charge of 2 μC and then immersing the film in acetic acid for 5 min. Selective removal of the PMMA phase was determined in prior studies [12].

3. Results

3.1. Stabilization of 50/50 films

Fig. 2 shows the surface (left column) and interface (right column) morphologies of 50/50 thin films annealed at 158 ± 2°C for 40 days. Each row shows the same sample before and after selective etching the PMMA-rich phase. The film thickness increases from the first to fifth row as: 9.6, 18, 60, 130, and 220 nm. At 9.6 nm, the surface displays large mounds which flatten as the thickness increases to 60 nm. As thickness continues to increase, the surface again roughens but with a different morphology. After etching, the interface morphologies at 9.6 and 18 nm show individual and interconnected mounds of the SAN-rich phase, respectively. A comparison of the surface and interface shows that the surface protrusions are caused by the SAN-rich droplets.

At an intermediate thickness of 60 nm, the surface and interface are relatively featureless, and the surface roughness is comparable to an as-cast film. Upon increasing the thickness to 130 and 220 nm, the SAN-rich phase (Fig. 2h and j) forms an interconnected morphology (light) punctured with columns of the PMMA-rich domains (dark). Fig. 2h and j show that the removed PMMA-rich domains are deep and wide and increase with increasing thickness. Based on their diameter, the surface mounds in Fig. 2g and i sit over the holes shown in Fig. 2h and j. As shown previously for 100 nm films, these surface mounds form as the surface, wetting layer grows (i.e. early stage) by hydrodynamic

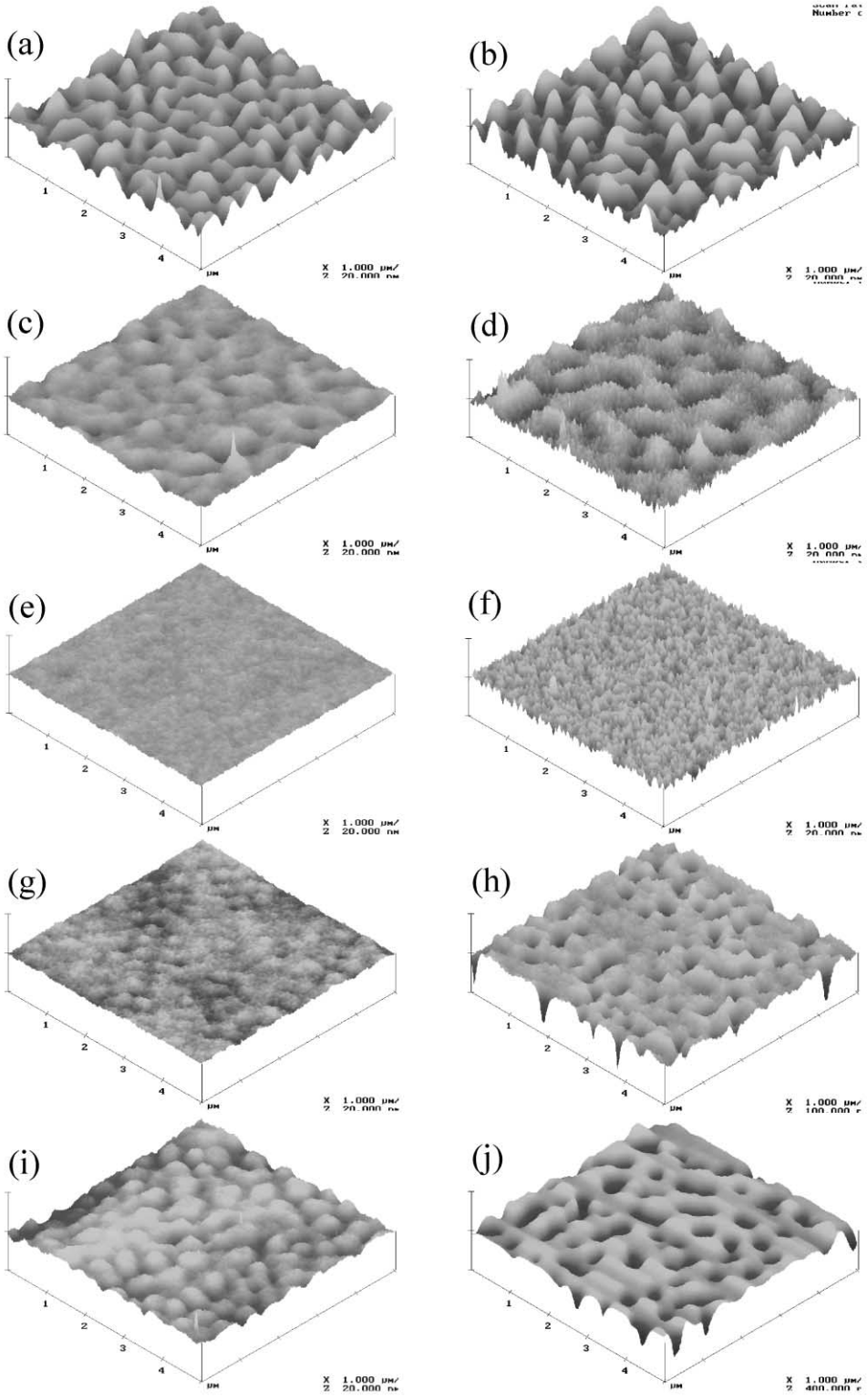

Fig. 2. The AFM scans of 50/50 PMMA/SAN blend films with various thicknesses annealed at 158 ± 2°C for 40 days. The images on the left and right columns are the same samples before and after removing the PMMA-rich phase, respectively. The film thicknesses for (a) and (b), (c) and (d), (e) and (f), (g) and (h), and (i) and (j) are: 9.6, 18, 60, 130, and 220 nm, respectively. The z-range for images (a)–(g), and (i) is 20 nm. The z-range ranges for (h) and (j) are 100 and 400 nm, respectively. All images are 5×5 μm.

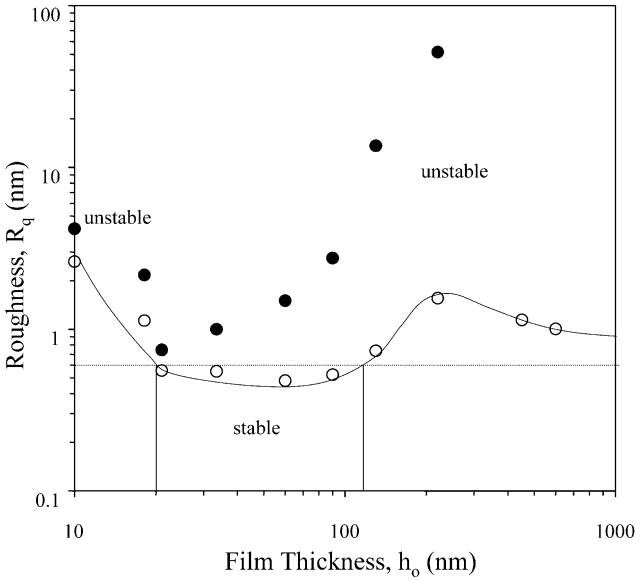

Fig. 3. The surface and interfacial roughness analyzed from the AFM scans shown in Fig. 2 are plotted against the original film thickness, h_0. The dashed line separates the stable films ($R_q < 0.6$ nm) from the unstable ones. Stable films are observed for thickness values ranging from 20 to 110 nm. The apparent roughness decreases for films thicker than 220 nm, because the phase dimension has become comparable to the scan size (5×5 μm).

flow of PMMA towards the surface. Qualitatively, Fig. 2 shows that a 50/50 blend is stable at 60 nm. However, films are unstable below and above this value because of film dewetting and phase separation of PMMA-rich domains within the middle layer, respectively. Next, we quantify this observation using surface and interfacial roughness values.

3.2. Stable and unstable films

For the 50/50 films shown in Fig. 2, the roughness of the surface and the interface are plotted as a function of film thickness in Fig. 3. Using the root mean square roughness (R_q) values, we can define, albeit in a subjective way, 'stable' and 'unstable' films. For very thin films, a large surface roughness ($R_q > 2$ nm) is observed. This roughness decreases from 2.6 nm to less than 0.6 nm as film thickness increases from 9.6 nm to about 20 nm. Small values of R_q are measured for thickness ranging from 20 nm to about 110 nm. Then the roughness increases again for films thicker than 110 nm. Although the interface is always rougher than the surface at a given thickness, the interfacial roughness follows a similar trend as the surface roughness. As shown in Fig. 3, the interfacial roughness decreases from about 4 nm at a film thickness of 10 nm to below 1 nm at a thickness of around 20 nm. The interfacial roughness increases slowly up to a thickness of around 100 nm and then rapidly beyond this thickness. For films with a surface roughness below 0.6 nm and an interfacial roughness less than 3 nm, the surface appears smooth and the interface is

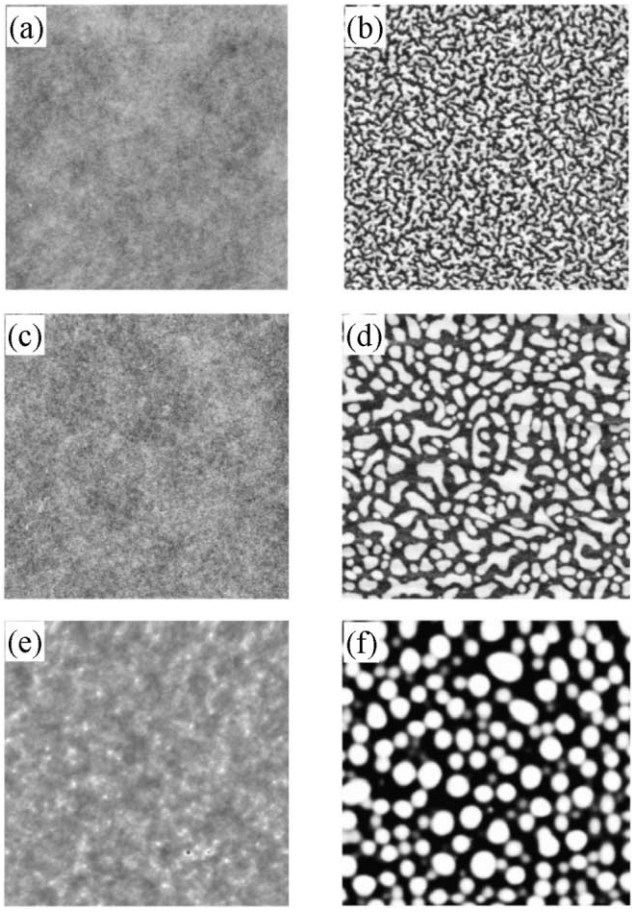

Fig. 4. This figure shows the AFM scans of the blends annealed at 166 ± 2°C for 15 days and with the PMMA-rich phase removed. The left and right columns are the 25/75 PMMA/SAN blend and the 75/25 PMMA/SAN blend, respectively. The film thickness of (a) and (b), (c) and (d), and (e) and (f) are 30, 60, and 220 nm.

devoid of mounds or droplets. We use these roughness conditions to define a stable film. Thus, for a 50/50 blend annealed at 158°C, films ranging from 20 to 110 nm thick are stable, whereas films thinner than 20 nm and thicker than 110 nm are unstable.

The surface and interface roughness of blend films with compositions of 25/75 and 75/25 are also measured. The 25/75 films maintain a smooth surface over a wide range of temperatures. However, the 75/25 blends, with film thickness ranging from 30 to 600 nm, display a surface roughness greater than 0.6 nm between 158 and 200°C. Fig. 4 shows the interfacial morphology of selected 25/75 (left column) and 75/25 (right column) films annealed at 166 ± 2°C for 15 days after etching PMMA. Fig. 4a–f correspond to thickness values of 30, 60, and 220 nm, respectively. The interfaces of the 25/75 films are relatively smooth with no noticeable domain formation. As film thickness increases, the interfacial roughness only increases slightly (i.e. 0.46, 0.73, and 2.2 nm, respectively). Because the surface roughness is less than 0.6 nm, these 25/75 films are stable.

On the other hand, under identical annealing conditions,

the 75/25 blends are unstable. The values of surface R_q are 2.7, 3.9 and 1.2 nm for thickness values of 30, 60, and 220 nm, respectively. After removing the PMMA-rich phase (right column), the raised domains (white) are observed, and the interface roughness significantly increases to 8.2, 12.8, and 24.2 nm, respectively. Based on the surface roughness, interfacial roughness and morphology, the 75/25 films are defined as unstable.

3.3. Stability diagram

Using the surface and interfacial roughness as a guide, a 'stability diagram' can be generated at each film thickness. Selected thickness values are shown in Fig. 5. In Fig. 5a–e, filled symbols denote unstable films, where the values of R_q for surface and interface are greater than 0.6 and 3 nm, respectively. The half-filled symbols correspond to films with a surface roughness below 0.6 nm, and an interfacial roughness between 0.6 and 3 nm. The open symbols represent films with both a surface and interface roughness below 0.6 nm. Both half-filled and open symbols correspond to stable films. For each diagram, the solid line separates the stable and unstable regimes. Fig. 5f shows the stability diagrams for the samples displayed in Fig. 5a–e. For all thickness values, the 75/25 films are unstable, even at a temperature of 158°C, which is 12°C below the bulk LCST. However, the 25/75 films are stable over a wide temperature range. Only at relatively high temperatures (>185°C), very thin (<30 nm) and thick (>220 nm) films are unstable, whereas at intermediate thickness values (i.e. 60 and 90 nm) films are stable even at temperatures as high as 200°C. Fig. 5 shows that the unstable region is largest for both thin (<30 nm) and thick (>220 nm) films, and smaller for films with intermediate thickness values (60–90 nm).

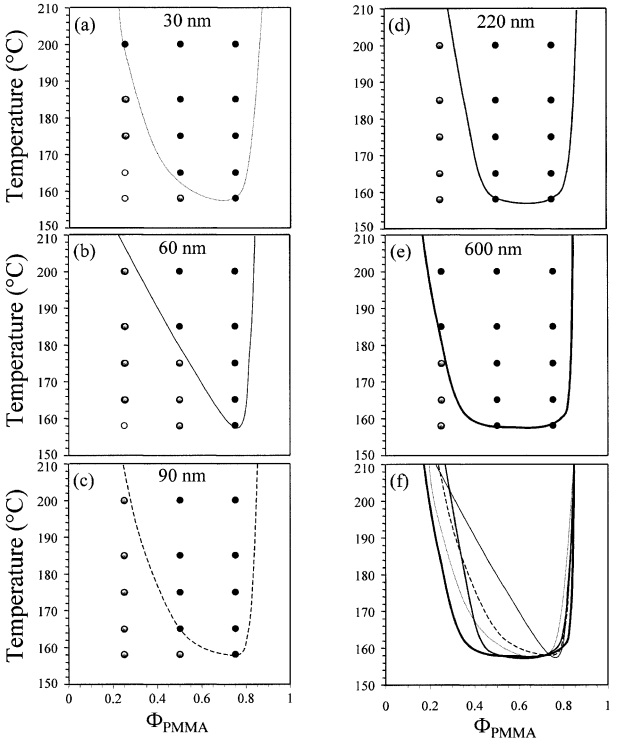

Fig. 5. The stability diagrams of PMMA/SAN thin films for thickness values of 30, 60, 90, 220, and 600 nm from (a) to (e). The filled symbols represent the unstable films, where the surface $R_q > 0.6$ nm and interfacial $R_q > 3$ nm. The half filled symbols denote the phase separated films that are stable; where the surface $R_q < 0.6$ nm, and interfacial 0.6 nm $< R_q < 3$ nm. The open symbols represent the stable films without phase separation; where both the surface and interfacial $R_q < 0.6$ nm. The lines drawn in the figures are guides to separate the stable and unstable regimes. (f) A comparison of the different thickness values.

3.4. Phase separation

The phase diagram of this blend is shifted slightly towards lower temperatures relative to the stability diagram. The phase separation is determined by comparing the roughness of the annealed and preannealed films before and after etching. The preannealed film shows similar values of R_q before and after etching. However, many annealed samples display an interfacial roughness that is greater than the surface roughness. Thus, films having the same interfacial and surface roughness are considered homogeneous; however, films are considered phase separated if the interfacial roughness is larger than the surface roughness. Both the filled and half-filled symbols shown in Fig. 5 represent the phase-separated films. In this study, phase separation is observed at temperatures as low as 158°C, which is 12°C below the bulk LCST. This observation suggests that thin film confinement acts to destabilize PMMA/SAN blends.

4. Discussion

4.1. Phase morphology and selective etching

Phase separation cannot be determined solely from the surface topography, but rather it is usually necessary to remove one component to reveal the underlying film morphology. For example, Fig. 6 shows that 220 nm thick 75/25 and 50/50 films annealed at 158°C both display surface features, in the former case dimples (Fig. 6a and the latter mounds (Fig. 6c). After selective etching of the PMMA-rich phase, the surface wetting layer is removed as well as the PMMA-rich phase below the surface. For the 75/25 film shown in Fig. 6b, the SAN-rich phase forms isolated droplets (white shapes) whereas the PMMA-rich phase (dark) forms an interconnected morphology. By contrast, in the 50/50 film, Fig. 6d shows that the PMMA-rich phase forms isolated channels (dark features) that puncture a continuous middle layer of the SAN-rich matrix (white). Therefore, the true phase morphology within the film can be observed only after removing the PMMA-rich phase. Removal of the PMMA-rich phase also allows one to determine the interfacial roughness, which is a measure of both film stability and phase separation.

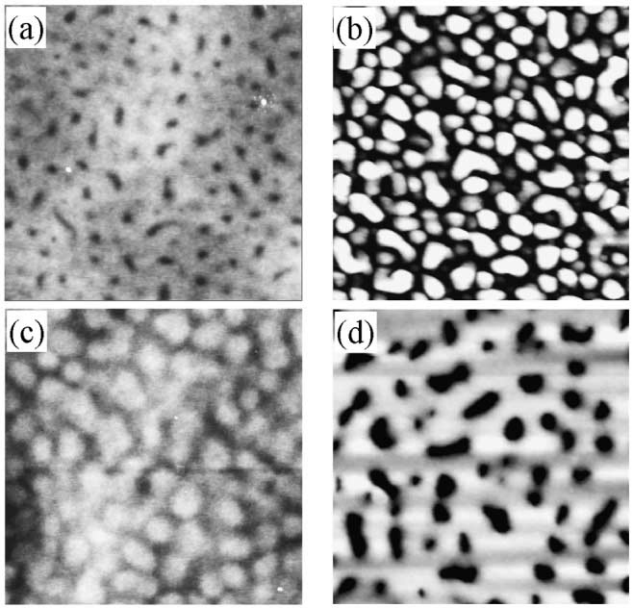

Fig. 6. The AFM topographies of the 75/25 films, (a) and (b), and the 50/50 films, (c) and (d), before, (a) and (c), and after, (b) and (d), the removal of the PMMA-rich phase. The films have been annealed inside a vacuum oven at 158 ± 2°C for 40 days.

4.2. Film stability analysis

Previous studies show that the PMMA-rich phase quickly wets both the substrate and air during phase separation, and a tri-layer structure, PMMA-rich/SAN-rich/PMMA-rich, initially forms. For a film to be stable, this layered structure must also be stable and resist capillary fluctuations at the interfaces. Recent studies [6,12] indicate that the wetting layer at the polymer/substrate interface, h_{w-sub}, is much thinner than the wetting layer at the polymer/air interface, h_{w-air}. For our analysis, we assume that h_{w-sub} is one monolayer thick (~8 nm for 91 K PMMA). For a very thin film, the tri-layer structure may initially form, but the film rapidly becomes unstable and dewets from the substrate. A detailed analysis of PMMA/SAN films less than or equal to 8 nm will be published shortly. For a 50/50 blend, Fig. 2a and b show large mounds in films less than 18 nm thick. For these films, even if all the PMMA molecules migrate to wet the substrate, not enough PMMA is available to form a monolayer, which covers the entire substrate. Because SAN alone dewets from SiOx, the blends eventually dewet the substrate and form droplets. At a film thickness of 18 nm, a monolayer (8 nm) of PMMA can form at the polymer/substrate interface. However if some PMMA molecules segregate to the surface, incomplete coverage of the PMMA molecules at the substrate will occur; thus dewetting can still occur for 18 nm films as shown in Fig. 2c and d.

For films thicker than 18 nm, a tri-layer structure is forms. The film is stable if h_{w-air} is less than the equilibrium wetting thickness; however, if the wetting layer reaches its equilibrium thickness and the concentration of PMMA in the middle SAN-rich layer is greater than the co-existing composition of PMMA, the middle SAN-rich layer will phase separate and eventually cause dewetting of the SAN-rich phase from the PMMA wetting layers. Therefore, the requirements for stable and unstable films are,

$$\text{stable}: \quad \phi_{\text{PMMA-mid}} = \phi'_{\text{PMMA}} \tag{1}$$

$$h_{w-air} \leq (h_{w-air})_e$$

$$\text{unstable}: \quad h_{w-air} = (h_{w-air})_e, \tag{2}$$

$$\phi_{\text{PMMA-mid}} > \phi'_{\text{PMMA}}$$

where $\phi_{\text{PMMA-mid}}$ is the volume fraction of PMMA (minority phase) in the SAN-rich middle layer (majority phase), ϕ'_{PMMA} is the co-existing volume fraction of PMMA minority phase, and $(h_{w-air})_e$ is the equilibrium wetting layer thickness at the air/polymer interface.

Studies performed by Wang [12] indicate that the value of $(h_{w-air})_e$ is about 0.4 of h_0, the initial film thickness, for 50/50 films less than 500 nm thick. Assuming a linear relationship between $(h_{w-air})_e$ and ϕ_{PMMA}, the values of $(h_{w-air})_e$ are taken as 0.2 h_0 and 0.6 h_0 for the 25/75 and 75/25 blends, respectively. For stable films, the middle SAN-rich layer has its co-existing composition and the value of h_{w-air} can be estimated by

$$h_{w-air} = \frac{(\phi_{\text{PMMA}} - \phi'_{\text{PMMA}})h_0}{(1 - \phi'_{\text{PMMA}})} - h_{w-sub}, \tag{3}$$

where ϕ_{PMMA} is the overall PMMA volume fraction in the blend and corresponds to 0.234, 0.478, and 0.733 for the samples 25/75, 50/50 and 75/25, respectively. Table 1 summarizes the stability criteria for each composition and thickness studied. For a 50/50 blend thicker than 18 nm but thinner than 110 nm, the PMMA molecules likely form a monolayer that covers the entire substrate and stabilizes the film. Over this thickness range, the surface wetting layer is starved of PMMA ($h_{w-air} < 0.4h_0$) and these films are predicted and experimentally observed to be stable. For the 130 nm thick film, h_{w-air} is about $0.39h_0$. Although $h_{w-air} < 0.4h_0$, experiments show that the film is unstable. This discrepancy is possibly due to the experimental uncertainty in determining $(h_{w-air})_e$, which may be slightly smaller. For the 25/75 films ranging from 30 to 600 nm in thickness, the value of h_{w-air} is less than $0.2h_0$; therefore these films are predicted to be stable up to 200°C. However, experimentally, the 600 nm films are unstable above 185°C. One possible explanation is that we have overestimated the value of $(h_{w-air})_e = 0.2h_0$; if a value of $0.18h_0$ were used, $\phi_{\text{PMMA-mid}}$ would be slightly greater than 0.05, the value of ϕ'_{PMMA} between 185 and 200°C [6]. In this case, after the formation of the tri-layer structure, the middle layer will phase separate and destablize the film.

We propose that an important mechanism for film destabilization is the dewetting of the SAN-rich phase from the PMMA-rich wetting layer after the tri-layer

Table 1
The values of ϕ_{PMMA} for the SAN-rich layer and the PMMA-wetting layer thickness at the polymer/air interface, h_{w-air}, for various PMMA/SAN blend thin films after being annealed. The equilibrium PMMA-rich wetting layer thickness at the air/polymer interface are taken as $0.2h_0$, $0.4h_0$ and $0.6h_0$ for 25/75, 50/50, and 75/25 blends, respectively, and the PMMA-rich layer at the polymer/substrate interface is one monolayer (~8 nm) thick. The co-existing composition, ϕ'_{PMMA} of 5 wt% is chosen based on previous studies [7] for films annealed between 185 and 200°C

wt % PMMA (initial blend)	h_0 (nm)	h_{w-sub} (nm)	h_{w-air} (nm)	h_{w-air}/h_0 (%)	wt% PMMA (in mid-layer of annealed blend)
25	30	~6	~0	0	Co-existing
	60	~8	~4	~7	Co-existing
	90	~8	~10	~11	Co-existing
	130	~8	~18	~14	Co-existing
	220	~8	~35	~16	Co-existing
	600	~8	~110	~18.3	Co-existing
50	9.6	~4.5	~0	0	Co-existing
	18	~8	< 1	~0	Co-existing
	30	~8	~6	~19	Co-existing
	60	~8	~19	~32	Co-existing
	90	~8	~34	~36	Co-existing
	110	~8	~44	~38	Co-existing
	130	~8	~52	~39	~3
	220	~8	~88	40	~7
	600	~8	~240	40	~11
75	30	~8	~14	~45	Co-existing
	60	~8	~35	~59	Co-existing
	90	~8	~54	~60	14
	130	~8	~78	~60	21
	220	~8	~132	~60	27
	600	~8	~360	~60	31

structure forms. If phase separation is to occur in the middle layer, the value of $\phi_{PMMA\text{-}mid}$ should be greater than that of ϕ'_{PMMA}. If the equilibrium wetting layer thickness is known, $\phi_{PMMA\text{-}mid}$ can be estimated from

$$\phi_{PMMA\text{-}mid} = \frac{\phi_{PMMA} h_0 - (h_{w-air})_e - h_{w-sub}}{h_0 - (h_{w-air})_e - h_{w-sub}} \quad (4)$$

As shown in Table 1, for the 50/50 blends equal to or greater than 220 nm, $\phi_{PMMA\text{-}mid}$ is greater than ϕ'_{PMMA}. This prediction agrees with the experimental observation of unstable films. The 75/25 blend films are unstable at all temperatures and over the entire thickness range, 30–600 nm. Using Eq. (4), $\phi_{PMMA\text{-}mid}$ is greater than ϕ'_{PMMA} for films thicker than 90 nm, but not for the 30 and 60 nm cases. However, if $(h_{w-air})_e$ was slightly underestimated, the unstable nature of the 60 nm film could be explained. For the 30 nm case, capillary fluctuations may be the destabilizing mechanism as proposed in a recent publication [13].

5. Concluding remarks

A thin film blend remains stable if phase separation and dewetting can be suppressed. In some cases, however, the films can remain stable if phase separation and wetting leads to a layered structure. In this study of PMMA/SAN films, we have observed film stability in a tri-layer structure if the middle SAN-rich layer has its co-existing composition, and the PMMA-rich surface wetting layer is less than or equal to its equilibrium thickness. For thicker films or those with high overall PMMA volume fraction, stabilization is directly related to phase separation. These films become unstable as the mid-layer ruptures and forms phase domains. Very thin blends (1–2 R_g) are always unstable because they undergo 2D phase separation and dewet from the substrate. Therefore, thin film stability can be enhanced by confining the film to a thickness of 3–5 R_g, or by reducing the PMMA volume fraction in thicker films.

For a thin film blend, such as PMMA/SAN, undergoing simultaneous wetting and phase separation, film stabilization can be improved by starving the wetting layer at the polymer/air interface. To extend this concept to other systems, the equilibrium wetting layer thickness at the polymer/air interface, $(h_{w-air})_e$, needs to be determined either experimentally or theoretically. In this study, we have assumed the values of (h_{w-air}) by extrapolating experimental measurements [12]. Although these values have some uncertainty, the predicted stability was in good agreement with a majority of the experimental observations. If the value of $(h_{w-air})_e$ could be precisely predicted or measured, thin film stability could be carefully controlled by selecting the optimum thickness and blend composition.

Several groups have used the spreading condition to predict interfacial roughening of thin film blends [14,15]. In this paper, a stability diagram was used to interpret phase

separation and dewetting in PMMA/SAN blends. Surprisingly, phase separation occurs for films at temperature less than the bulk LCST suggesting that confinement destabilizes the film in contrast to theoretical studies [2,3]. This study also demonstrates that selective etching in combination with AFM is a very sensitive method for revealing the phase morphology of polymer blends.

Acknowledgements

We acknowledge primary financial support from NSF DMR (9974366) and NSF MRSEC (DMR00-79909) program. SEF were supported by NSF MRSEC. This paper is dedicated to Professor R.S. Stein for his research accomplishments that helped establish the field of physical polymer science, and his educational and mentorship contributions to many generations of polymer scientists.

References

[1] Wang H, Composto RJ. Europhys Lett 2000;50:622.
[2] Tang H, Szleifer I, Kumar SK. J Chem Phys 1994;100:5367.
[3] Reich S, Cohen Y. J Polym Sci Polym Phys 1981;19:1255.
[4] Binder K. J Non-Equilib Thermodyn 1998;23:1.
[5] Oslanec R. Ph.D. dissertation, University of Pennsylvania, 1997.
[6] Zhang Newby B, Composto RJ. Macromolecules 2000;33:3274.
[7] McMaster LP. Macromolecules 1973;6:760.
[8] Suess M, Kressler J, Kammer HW. Polymer 1987;28:957.
[9] Fowler ME, Barlow JW, Paul DR. Polymer 1987;28:1177.
[10] Higashida N, Kressler J, Yukioka S, Inoue T. Macromolecules 1992;25:5259.
[11] Madbouly SA, Ougizawa T, Inoue T. Macromolecules 1999;32:5631.
[12] Wang H. Ph.D. dissertation, University of Pennsylvania, 1999.
[13] Wang H, Composto RJ, Hobbie EK, Han CC. Langmuir 2001;17:2857.
[14] Karim A, Slawecki TM, Kumar SK, Douglas JF, Satija SK, Han CC, Russell TP, Lui Y, Overney R, Sokolov J, Rafailovich MH. Macromolecules 1998;31:857 (and references therein).
[15] Affrossman S, O'Neill SA, Stamm M. Macromolecules 1998;31:6280 (and references therein).